Photoproduction in Ultra-Peripheral Relativistic Heavy Ion Collisions at STAR

Boris Grube

Pusan National University
Department of Physics
Busan, Republic of Korea

Brookhaven National Laboratory
Upton, NY, U.S.A.

eRHIC Meeting
BNL, August 14th, 2008

PUSAN NATIONAL UNIVERSITY

BROOKHAVEN NATIONAL LABORATORY

Outline

1. Ultra-peripheral relativistic heavy ion collisions at STAR
2. Triggering and data selection
3. Some results on photonuclear ρ production in Au $\times$ Au collisions

Outline

Ultra-Peripheral Heavy Ion Collisions (UPC) at STAR

- Nuclei surrounded by cloud of quasi-real virtual photons
- Number of photons large ($\propto Z^2$)
- Fast-moving heavy ions produce intense photon flux
  - Described by Weizsäcker-Williams approximation ("nuclear flashlight")
- Nuclear collisions: long range interaction via electromagnetic fields in addition to hadronic interactions
- Require $b > R_A + R_B$ to exclude (otherwise inseparable) hadronic interactions

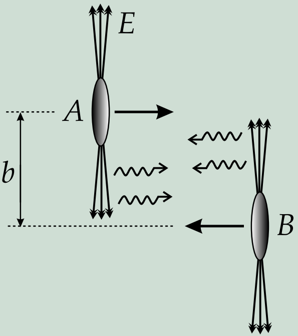

Ultra-Peripheral Relativistic Heavy Ion Collisions (UPC)

Three basic interaction processes

1. Photon-photon interactions

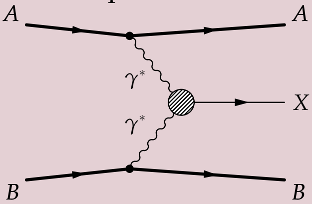

2. Photonuclear interactions

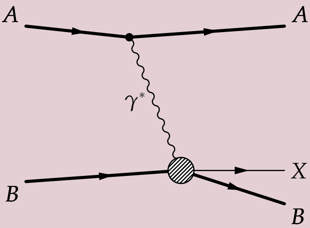

3. Nuclear breakup

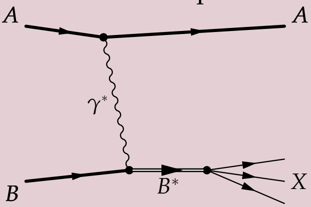

Ultra-Peripheral Relativistic Heavy Ion Collisions (UPC)

UPC kinematics for RHIC Au $\times$ Au @ $\sqrt{s_{NN}} = 200$ GeV and LHC Pb $\times$ Pb @ $\sqrt{s_{NN}} = 5500$ GeV

- Photons emitted coherently by whole nucleus
- Maximum photon energy in lab frame: $\omega_{\max} = \gamma_L \hbar c / R_A$
  $\omega_{\max} \approx 3\,\text{GeV (RHIC)}, 80\,\text{GeV (LHC)}$
- Photon-photon collisions: $\sqrt{s_{\gamma\gamma}^{\max}} = 2\gamma_L \hbar c / R_A$
  $\sqrt{s_{\gamma\gamma}^{\max}} \approx 6\,\text{GeV (RHIC)}, 160\,\text{GeV (LHC)}$
- Photonuclear interactions: $\sqrt{s_{\gamma N}^{\max}} = \sqrt{2\omega_{\max}\sqrt{s_{NN}}}$
  $\sqrt{s_{\gamma N}^{\max}} \approx 35\,\text{GeV (RHIC)}, 950\,\text{GeV (LHC)}$

Ultra-Peripheral Heavy Ion Collisions (UPC) at STAR

UPC processes measured at STAR

1. **Photonuclear interactions**
   - ρ production in Au $\times$ Au @ $\sqrt{s_{NN}} = 200$, and 130 GeV
   - γ^* from "spectator" ion fluctuates into $q\bar{q}$-pair
   - $q\bar{q}$-pair scatters off "target" nucleus into real vector meson
   - Scattering described in terms of soft Pomeron exchange

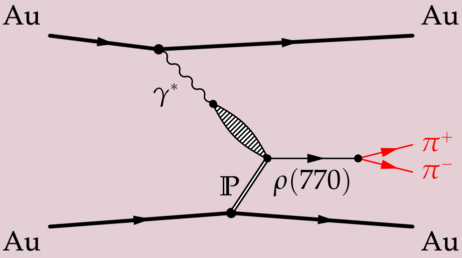

Ultra-Peripheral Heavy Ion Collisions (UPC) at STAR

UPC processes measured at STAR (cont.)

2. **Photonuclear interactions with mutual nuclear breakup**
   - ρ production in Au $\times$ Au @ $\sqrt{s_{NN}} = 200, 130$, and 62 GeV
   - Mutual Coulomb excitation of nuclei by additional photons
     - Independent of meson production
     - Predominantly excitation of Giant Dipole Resonance (GDR)
     - GDRs decay via neutron emission $\Longrightarrow$ distinctive signature

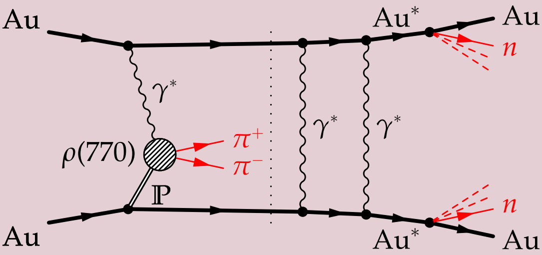

Ultra-Peripheral Heavy Ion Collisions (UPC) at STAR

UPC processes measured at STAR (cont.)

3. **Photon-photon interactions with mutual nuclear breakup**
   - e^+e^--pair production in Au $\times$ Au @ $\sqrt{s_{NN}} = 200$ GeV

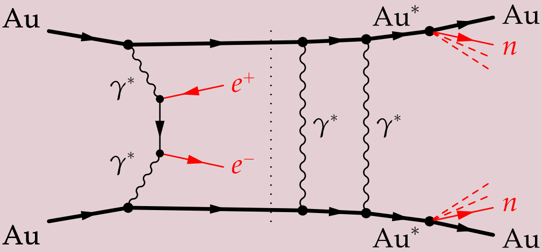

Outline

Triggering and Data Selection

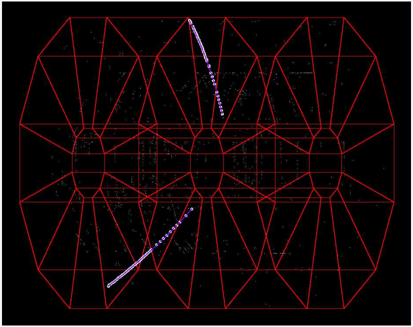

TPC tracks for typical ρ event

Experimental signature and event selection

- Coherent production dominates: particles produced in $\gamma^*\gamma^*$ and $\gamma^*\mathbb{P}$ have low $p_T \lesssim 2\hbar/R_A \approx 60$ MeV/c
- 2 well reconstructed tracks
  - From common vertex
  - Opposite charge
  - Low net p_T
- Vertex position close to interaction diamond
- Low overall track multiplicity
- For nuclear breakup: additional forward neutrons $\Longrightarrow$ trigger

STAR acceptance limits accessible rapidities to $|y| < 1$

Triggering and Data Selection

Trigger detectors

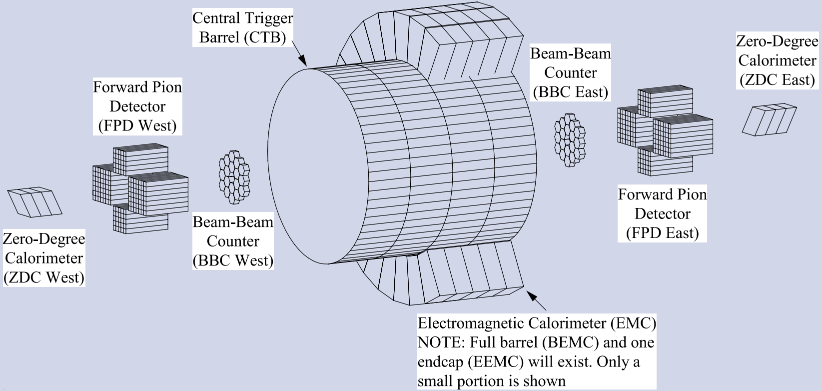

Triggering and Data Selection — Neutron tagging

Measuring nuclear breakup neutrons in Zero Degree Calorimeter (ZDC)

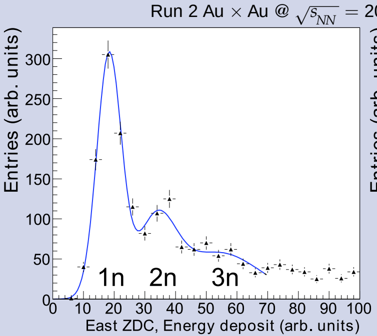

- ZDC acceptance for emitted neutrons close to 1
- Resolution good enough to see $1n, 2n, \ldots$ neutron peaks
  - Allows to select different excited states
- Neutron tag selects smaller impact parameters

Triggering and Data Selection

UPC triggers used at STAR

1. **Topology trigger** (CTB only)
   - CTB is subdivided into 4 quadrants
   - Top+Bottom quadrants veto cosmic rays
   - Coincidence of North and South quadrants
   - In addition low multiplicity requirement
   - **Does not require nuclear breakup**
2. **Minimum bias trigger** (ZDC only)
   - Coincident neutrons in both ZDCs

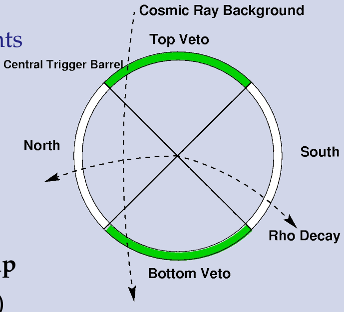

Triggering and Data Selection

UPC triggers used at STAR

3. **Multi-prong trigger** (CTB and ZDC)
   - Coincident neutrons in both ZDCs
   - Low CTB multiplicity
   - Veto from large-tile BBCs
4. ***J/ψ* trigger** (CTB, ZDC, and BEMC)
   - Multi-prong trigger with additional calorimeter requirement
   - BEMC subdivided into 6 azimuthal sectors
   - 2 high towers in non-neighboring BEMC sectors required

Triggering and Data Selection

Main background contributions

1. **Beam-gas interactions** reduced by
   - Requiring low track multiplicity
   - Limiting primary vertex position
2. **Peripheral hadronic interactions** reduced by
   - Requiring low track multiplicity
   - Selecting low p_T
3. **Pile-up events** reduced by
   - Requiring low track multiplicity
   - Limiting primary vertex position
4. **Cosmic rays** reduced by
   - Limiting primary vertex position
   - Either ZDC neutron tag or excluding events close to $|y| = 0$

Triggering and Data Selection

Main background contributions

1. **Beam-gas interactions** reduced by
   - Requiring low track multiplicity
   - Limiting primary vertex position
2. **Peripheral hadronic interactions** reduced by
   - Requiring low track multiplicity
   - Selecting low p_T
3. **Pile-up events** reduced by
   - Requiring low track multiplicity
   - Limiting primary vertex position
4. **Cosmic rays** reduced by
   - Limiting primary vertex position
   - Either ZDC neutron tag or excluding events close to $|y| = 0$

Triggering and Data Selection

Main background contributions

1. **Beam-gas interactions** reduced by
   - Requiring low track multiplicity
   - Limiting primary vertex position
2. **Peripheral hadronic interactions** reduced by
   - Requiring low track multiplicity
   - Selecting low p_T
3. **Pile-up events** reduced by
   - Requiring low track multiplicity
   - Limiting primary vertex position
4. **Cosmic rays** reduced by
   - Limiting primary vertex position
   - Either ZDC neutron tag or excluding events close to $|y| = 0$

Triggering and Data Selection

Main background contributions

1. **Beam-gas interactions** reduced by
   - Requiring low track multiplicity
   - Limiting primary vertex position
2. **Peripheral hadronic interactions** reduced by
   - Requiring low track multiplicity
   - Selecting low p_T
3. **Pile-up events** reduced by
   - Requiring low track multiplicity
   - Limiting primary vertex position
4. **Cosmic rays** reduced by
   - Limiting primary vertex position
   - Either ZDC neutron tag or excluding events close to $|y| = 0$

Triggering and Data Selection

Main background contributions

1. **Beam-gas interactions** reduced by
   - Requiring low track multiplicity
   - Limiting primary vertex position
2. **Peripheral hadronic interactions** reduced by
   - Requiring low track multiplicity
   - Selecting low p_T
3. **Pile-up events** reduced by
   - Requiring low track multiplicity
   - Limiting primary vertex position
4. **Cosmic rays** reduced by
   - Limiting primary vertex position
   - Either ZDC neutron tag or excluding events close to $|y| = 0$

Outline

ρ Production Cross Section

Run 1 Au $\times$ Au @ $\sqrt{s_{NN}} = 130$ GeV data

p_T^{ρ} spectrum (Min. Bias)

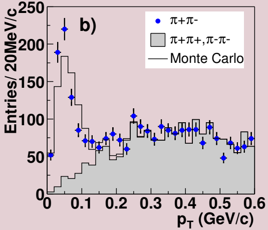

Rapidity distribution (Min. Bias)

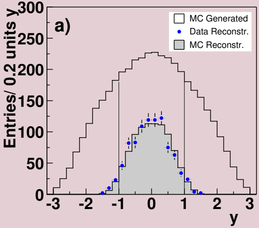

$d\sigma / dM_{\pi\pi}$ (Min. Bias)

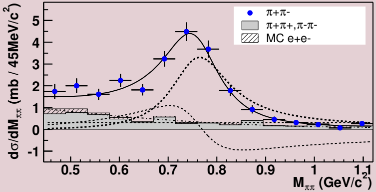

- Total cross section: $\sigma_{\text{tot}} = (460 \pm 220_{\text{stat.}} \pm 110_{\text{sys.}})$ mb
  PRL **89**, 272302 (2002)
- Theoretical prediction: $\sigma_{\text{tot}} = 350$ mb
  S. Klein *et al.*, PR **C60**, 014903 (1999)

t-Dependence of ρ Production Cross Section

Run 2 Au $\times$ Au @ $\sqrt{s_{NN}} = 200$ GeV data

PR **C77**, 34910 (2008)

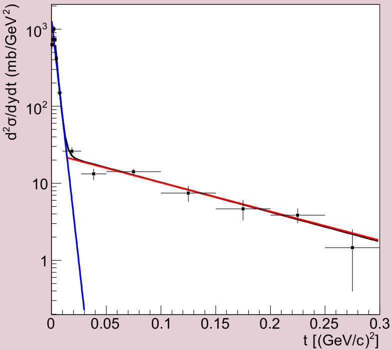

Parameterization: $$\left.\frac{d\sigma_\rho}{dt}\right|_{|y_\rho|<1} = A_{\text{coh}}\, e^{-B_{\text{coh}} \cdot t} + A_{\text{inc}}\, e^{-B_{\text{inc}} \cdot t}$$

- Coherent slope parameter $B_{\text{coh}} = 388 \pm 24\,(\text{GeV}/c)^{-2}$
- Incoherent slope parameter $B_{\text{inc}} = 8.8 \pm 1.0\,(\text{GeV}/c)^{-2}$

Outline

4 Backup slides

- STAR detector
- Results on photonuclear ρ production in Au $\times$ Au collisions
  - ρ production cross section
  - Spin structure of ρ production amplitudes
  - Interference effects in coherent ρ production
- Other results
  - Photonuclear ρ production in d $\times$ Au collisions
  - $\pi^+\pi^-\pi^+\pi^-$ production in Au $\times$ Au collisions
  - e^+e^--pair production in Au $\times$ Au collisions

The STAR Experiment at RHIC

Detector components important for UPC measurements Nucl. Instr. Meth. **A499**

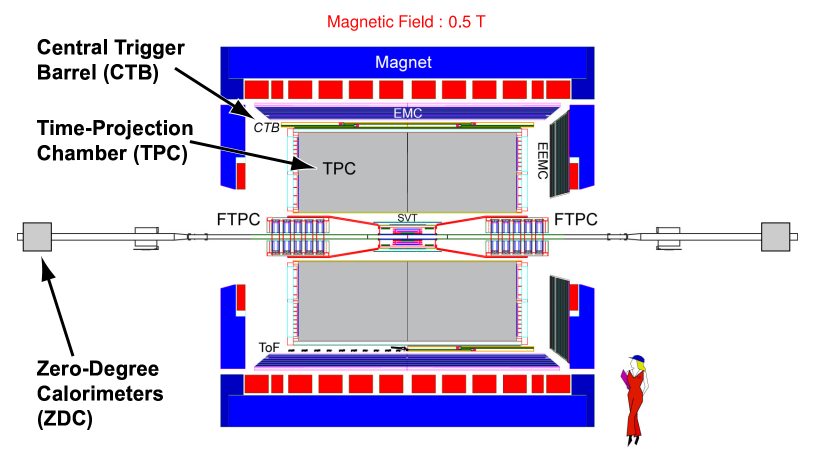

Star Upgrades for 2009+

Time of Flight (ToF) Detector

- Replaces central trigger barrel
- Multi-gap resistive plate chambers (MRPC) using ALICE technology
- 23 000 channels (6 slats $\times$32 plates $\times$120 trays)
- Full coverage of TPC acceptance (2π in ϕ, $|\eta| < 1$)
- Intrinsic time resolution $\approx$ 85 ps

Upgrade of data acquisition (DAQ)

- New TPC front-end electronics based on ALICE's ALTRO chip
- Will permit trigger rates $\mathcal{O}(1\,\text{kHz}) \implies$ DAQ1000

ρ Yield from Run 2 Au $\times$ Au @ $\sqrt{s_{NN}} = 200$ GeV

2 trigger sets

1. **Topology trigger**
   - No nuclear breakup required
   - $13\,054 \pm 124$ ρ candidates
2. **Minimum bias trigger**
   - ZDC neutron tag
   - $3\,075 \pm 128$ ρ candidates

- Background estimate from like-sign pairs $\pi^\pm\pi^\pm$

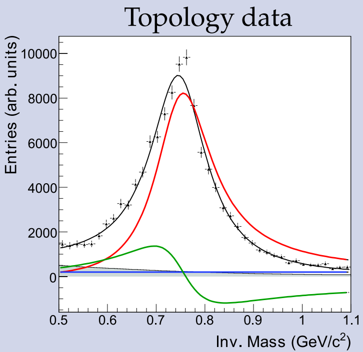

PR **C77**, 034910 (2008)

ρ Yield from Run 2 Au $\times$ Au @ $\sqrt{s_{NN}} = 200$ GeV

2 trigger sets

1. **Topology trigger**
   - No nuclear breakup required
   - $13\,054 \pm 124$ ρ candidates
2. **Minimum bias trigger**
   - ZDC neutron tag
   - $3\,075 \pm 128$ ρ candidates

- Background estimate from like-sign pairs $\pi^{\pm}\pi^{\pm}$

Minimum bias data

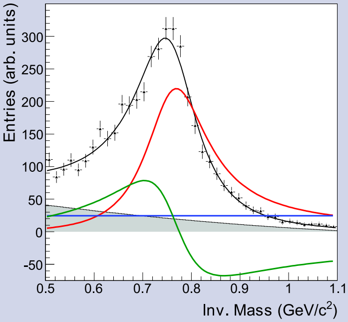

PR **C77**, 034910 (2008)

ρ Invariant Mass Fit

Fit function with 4 components

$$\frac{d\sigma}{dM_{\pi\pi}} = \left| A \frac{\sqrt{M_{\pi\pi} M_\rho \Gamma}}{M_{\pi\pi}^2 - M_\rho^2 + i M_\rho \Gamma} + B \right|^2 + f_{BG}$$

$$\text{with } \Gamma(M_{\pi\pi}) \equiv \Gamma_\rho \frac{M_\rho}{M_{\pi\pi}} \left[\frac{M_{\pi\pi}^2 - 4m_\pi^2}{M_\rho^2 - 4m_\pi^2} \right]^{\frac{3}{2}}$$

1. Relativistic Breit-Wigner function for ρ peak with amplitude A
2. Constant direct $\pi^+\pi^-$ production amplitude B
3. Söding term for interference of the two
4. 2nd order polynomial f_{BG} describes background from like-sign pairs

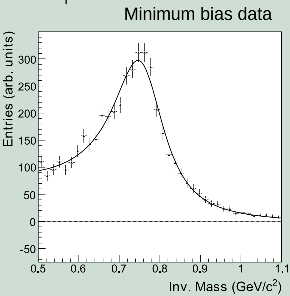

ρ Invariant Mass Fit

Fit function with 4 components

$$\frac{d\sigma}{dM_{\pi\pi}} = \left| A \frac{\sqrt{M_{\pi\pi} M_\rho \Gamma}}{M_{\pi\pi}^2 - M_\rho^2 + i M_\rho \Gamma} + B \right|^2 + f_{BG}$$

$$\text{with } \Gamma(M_{\pi\pi}) \equiv \Gamma_\rho \frac{M_\rho}{M_{\pi\pi}} \left[\frac{M_{\pi\pi}^2 - 4m_\pi^2}{M_\rho^2 - 4m_\pi^2} \right]^{\frac{3}{2}}$$

1. Relativistic Breit-Wigner function for ρ peak with amplitude A
2. Constant direct $\pi^+\pi^-$ production amplitude B
3. Söding term for interference of the two
4. 2nd order polynomial f_{BG} describes background from like-sign pairs

Minimum bias data

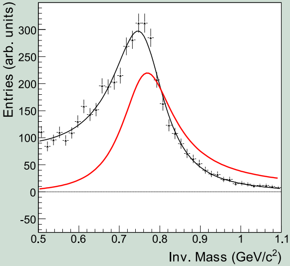

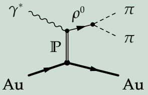

ρ Invariant Mass Fit

Fit function with 4 components

$$\frac{d\sigma}{dM_{\pi\pi}} = \left| A \frac{\sqrt{M_{\pi\pi} M_\rho \Gamma}}{M_{\pi\pi}^2 - M_\rho^2 + i M_\rho \Gamma} + B \right|^2 + f_{BG}$$

$$\text{with } \Gamma(M_{\pi\pi}) \equiv \Gamma_\rho \frac{M_\rho}{M_{\pi\pi}} \left[\frac{M_{\pi\pi}^2 - 4m_\pi^2}{M_\rho^2 - 4m_\pi^2} \right]^{\frac{3}{2}}$$

1. Relativistic Breit-Wigner function for ρ peak with amplitude A
2. Constant direct $\pi^+\pi^-$ production amplitude B
3. Söding term for interference of the two
4. 2nd order polynomial f_{BG} describes background from like-sign pairs

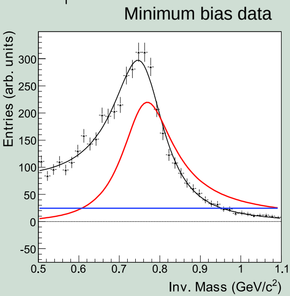

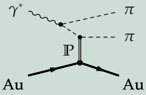

ρ Invariant Mass Fit

Fit function with 4 components

$$\frac{\mathrm{d}\sigma}{\mathrm{d}M_{\pi\pi}} = \left| A \frac{\sqrt{M_{\pi\pi} M_\rho \Gamma}}{M_{\pi\pi}^2 - M_\rho^2 + i M_\rho \Gamma} + B \right|^2 + f_{\mathrm{BG}}$$

$$\text{with } \Gamma(M_{\pi\pi}) \equiv \Gamma_\rho \frac{M_\rho}{M_{\pi\pi}} \left[\frac{M_{\pi\pi}^2 - 4m_\pi^2}{M_\rho^2 - 4m_\pi^2} \right]^{\frac{3}{2}}$$

1. Relativistic Breit-Wigner function for ρ peak with amplitude A
2. Constant direct $\pi^+\pi^-$ production amplitude B
3. Söding term for interference of the two
4. 2nd order polynomial f_{BG} describes background from like-sign pairs

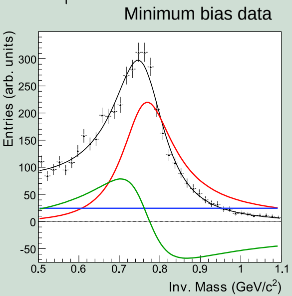

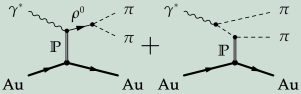

ρ Invariant Mass Fit

Fit function with 4 components

$$\frac{d\sigma}{dM_{\pi\pi}} = \left| A \frac{\sqrt{M_{\pi\pi} M_\rho \Gamma}}{M_{\pi\pi}^2 - M_\rho^2 + i M_\rho \Gamma} + B \right|^2 + f_{BG}$$

$$\text{with } \Gamma(M_{\pi\pi}) \equiv \Gamma_\rho \frac{M_\rho}{M_{\pi\pi}} \left[\frac{M_{\pi\pi}^2 - 4m_\pi^2}{M_\rho^2 - 4m_\pi^2} \right]^{\frac{3}{2}}$$

1. Relativistic Breit-Wigner function for ρ peak with amplitude A
2. Constant direct $\pi^+\pi^-$ production amplitude B
3. Söding term for interference of the two
4. 2nd order polynomial f_{BG} describes background from like-sign pairs

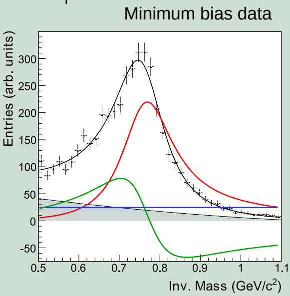

Direct $\pi^+\pi^-$ vs. ρ Production

Ratio of non-resonant to resonant $\pi^+\pi^-$ production

$$\frac{d\sigma}{dM_{\pi\pi}} = \left| A \frac{\sqrt{M_{\pi\pi} M_\rho \Gamma}}{M_{\pi\pi}^2 - M_\rho^2 + i M_\rho \Gamma} + B \right|^2 + f_{BG}$$

- Amplitudes A and B are fit parameters
- B/A measure for ratio of non-resonant to resonant $\pi^+\pi^-$ production
  - For Au $\times$ Au @ $\sqrt{s_{NN}} = 200$ GeV :
    $|B/A| = 0.89 \pm 0.08_{\text{stat.}} \pm 0.09_{\text{syst.}}$ GeV$^{-\frac{1}{2}}$
  - No dependence on angles or rapidity
    PR **C77**, 034910 (2008)
  - For Au $\times$ Au @ $\sqrt{s_{NN}} = 130$ GeV :
    $|B/A| = 0.81 \pm 0.08_{\text{stat.}} \pm 0.20_{\text{syst.}}$ GeV$^{-\frac{1}{2}}$
    PRL **89**, 272302 (2002)
  - In agreement with ZEUS EPJ **C2**, 247 (1998)

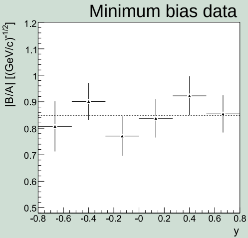

Direct $\pi^+\pi^-$ vs. ρ Production

Ratio of non-resonant to resonant $\pi^+\pi^-$ production

$$\frac{\mathrm{d}\sigma}{\mathrm{d}M_{\pi\pi}} = \left| A \frac{\sqrt{M_{\pi\pi} M_\rho \Gamma}}{M_{\pi\pi}^2 - M_\rho^2 + i M_\rho \Gamma} + B \right|^2 + f_{\mathrm{BG}}$$

- Amplitudes A and B are fit parameters
- B/A measure for ratio of non-resonant to resonant $\pi^+\pi^-$ production
  - For Au $\times$ Au @ $\sqrt{s_{NN}} = 200$ GeV :
    $|B/A| = 0.89 \pm 0.08_{\text{stat.}} \pm 0.09_{\text{syst.}}\ \mathrm{GeV}^{-\frac{1}{2}}$
  - No dependence on angles or rapidity
    PR **C77**, 034910 (2008)
  - For Au $\times$ Au @ $\sqrt{s_{NN}} = 130$ GeV :
    $|B/A| = 0.81 \pm 0.08_{\text{stat.}} \pm 0.20_{\text{syst.}}\ \mathrm{GeV}^{-\frac{1}{2}}$
    PRL **89**, 272302 (2002)
  - In agreement with ZEUS EPJ **C2**, 247 (1998)

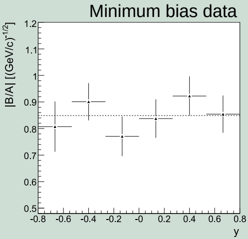

ρ Production Cross Section

Total ρ production cross section for Au $\times$ Au @ $\sqrt{s_{NN}} = 200$ GeV

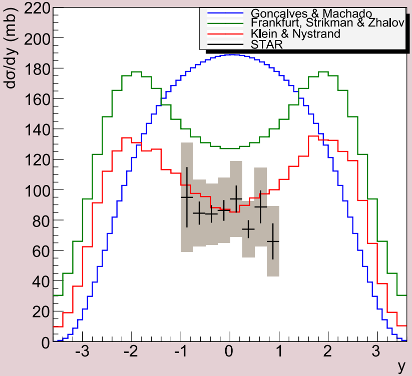

- σ_{tot} obtained by scaling $\sigma_{\text{mb}}(\text{nucl. breakup})$ from minimum bias data with ratio $\frac{\sigma_{\text{topo}}(\text{no nucl. breakup})}{\sigma_{\text{topo}}(\text{nucl. breakup})}$ from topology data

ρ Production Cross Section

Comparison with model predictions for Au $\times$ Au @ $\sqrt{s_{NN}} = 200$ GeV

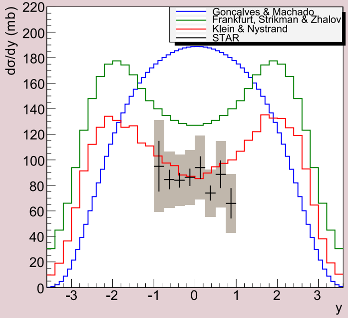

1. **Klein, Nystrand** PR **C60**, 014903 (1999)
   - Vector Dominance Model (VDM) for $\gamma^* \to |q\bar{q}\rangle$
   - Classical mechanical approach for scattering
   - Uses photoproduction data from $\gamma p \to \rho p$ experiments
2. **Frankfurt, Strikman, Zhalov** PR **C67**, 034901 (2003)
   - generalized VDM
   - QCD Gribov-Glauber approach
3. **Gonçalves, Machado** EPJ **C29**, 271-275 (2003)
   - QCD color dipole approach
   - Includes nuclear effects and parton saturation phenomena

ρ Production Cross Section

Energy dependence of coherent ρ production with nuclear breakup

- Based on total hadronic cross section of 7.2 b
- For **run 1** Au $\times$ Au @ $\sqrt{s_{NN}} = 130$ GeV
  $\sigma^{coh}_{XnXn} = 28.3 \pm 2.0_{stat.} \pm 6.3_{syst.}$ mb — PRL **89**, 272302 (2002)
- For **run 2** Au $\times$ Au @ $\sqrt{s_{NN}} = 200$ GeV
  $\sigma^{coh}_{XnXn} = 31.9 \pm 1.5_{stat.} \pm 4.5_{syst.}$ mb — PR **C77**, 034910 (2008)
- Currently analyzing **run 4**
  Au $\times$ Au @ $\sqrt{s_{NN}} = 62$ GeV
  data to get third data point

ρ Production Cross Section

Energy dependence of coherent ρ production with nuclear breakup

- Based on total hadronic cross section of 7.2 b
- For **run 1** Au $\times$ Au @ $\sqrt{s_{NN}} = 130$ GeV
  $\sigma^{coh}_{XnXn} = 28.3 \pm 2.0_{stat.} \pm 6.3_{syst.}$ mb — PRL **89**, 272302 (2002)
- For **run 2** Au $\times$ Au @ $\sqrt{s_{NN}} = 200$ GeV
  $\sigma^{coh}_{XnXn} = 31.9 \pm 1.5_{stat.} \pm 4.5_{syst.}$ mb — PR **C77**, 034910 (2008)
- Currently analyzing **run 4**
  Au $\times$ Au @ $\sqrt{s_{NN}} = 62$ GeV
  data to get third data point

Minimum bias data

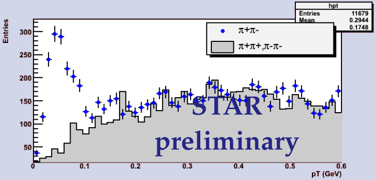

Spin Structure of ρ Production Amplitudes

Extraction of spin density matrix elements from $\pi^+\pi^-$ angular distribution

Schilling, Wolf NP **B61**, 381 (1973)

$$\frac{1}{\sigma}\frac{d^2\sigma}{d\cos\theta\, d\phi} = \frac{3}{4\pi}\left[\frac{1}{2}(1 - r^{04}_{00}) + \frac{1}{2}(3r^{04}_{00} - 1)\cos^2\theta - \sqrt{2}\,\Re\mathfrak{e}[r^{04}_{10}]\sin 2\theta\cos\phi - r^{04}_{1-1}\sin^2\theta\cos 2\phi\right]$$

- ρ production plane difficult to reconstruct
- Approximate production plane using beam direction
  - θ is polar angle between beam direction and $\vec{p}_{\pi^+}$ in ρ RF
  - ϕ is angle between ρ decay and production plane (w.r.t. beam)
- Due to ambiguity in beam direction cannot measure $\Re\mathfrak{e}[r^{04}_{10}]$ (interference between helicity non-flip and single-flip)

Spin Structure of ρ Production Amplitudes

Spin density matrix elements from fit of 2D angular distributions

1D projections of 2D angular distribution (minimum bias data)

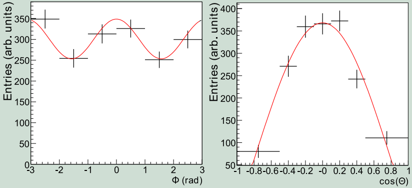

Parameter	STAR	ZEUS
r^{04}_{00}	$-0.03 \pm 0.03_{\text{stat.}} \pm 0.06_{\text{syst.}}$	$0.01 \pm 0.01_{\text{stat.}} \pm 0.02_{\text{syst.}}$
$\mathfrak{Re}[r^{04}_{10}]$	—	$0.01 \pm 0.01_{\text{stat.}} \pm 0.01_{\text{syst.}}$
r^{04}_{1-1}	$-0.01 \pm 0.03_{\text{stat.}} \pm 0.05_{\text{syst.}}$	$-0.01 \pm 0.01_{\text{stat.}} \pm 0.01_{\text{syst.}}$

- Results similar to ZEUS measurements EPJ **C2**, 247 (1998)
- Spin density elements close to zero indicate *s*-channel helicity conservation

Spin Structure of ρ Production Amplitudes

Spin density matrix elements from fit of 2D angular distributions

1D projections of 2D angular distribution (minimum bias data)

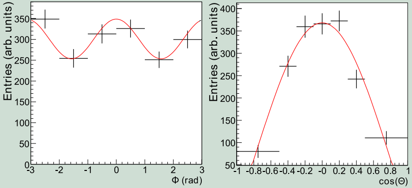

Parameter	STAR	ZEUS
r^{04}_{00}	$-0.03 \pm 0.03_{\text{stat.}} \pm 0.06_{\text{syst.}}$	$0.01 \pm 0.01_{\text{stat.}} \pm 0.02_{\text{syst.}}$
$\mathfrak{Re}[r^{04}_{10}]$	—	$0.01 \pm 0.01_{\text{stat.}} \pm 0.01_{\text{syst.}}$
$r^{04}_{1\,-1}$	$-0.01 \pm 0.03_{\text{stat.}} \pm 0.05_{\text{syst.}}$	$-0.01 \pm 0.01_{\text{stat.}} \pm 0.01_{\text{syst.}}$

- Results similar to ZEUS measurements EPJ **C2**, 247 (1998)
- Spin density elements close to zero indicate s-channel helicity conservation

Spin Structure of ρ Production Amplitudes

Extraction of spin density matrix elements from $\pi^+\pi^-$ angular distribution

$$\frac{1}{\sigma}\frac{d^2\sigma}{d\cos\theta\, d\phi} = \frac{3}{4\pi}\left[\frac{1}{2}(1 - r^{04}_{00}) + \frac{1}{2}(3r^{04}_{00} - 1)\cos^2\theta - \sqrt{2}\,\mathfrak{Re}[r^{04}_{10}]\sin 2\theta\cos\phi - r^{04}_{1\,-1}\sin^2\theta\cos 2\phi\right]$$

where $r^{04}_{ik} \equiv \frac{\rho^0_{ik} + \epsilon R\,\rho^4_{ik}}{1 + \epsilon R}$, $R = \frac{\sigma_L}{\sigma_T}$ Schilling, Wolf NP **B61**, 381 (1973)

- θ is polar angle between beam direction and $\vec{p}_{\pi^+}$ in ρ RF
- ϕ is angle between ρ decay and production plane (w.r.t. beam)
- r^{04}_{00} represents probability that $\lambda_\rho = 0$ for $\lambda_{\gamma^*} = \pm 1$
- $\mathfrak{Re}[r^{04}_{10}]$ related to interference between helicity non-flip and single-flip
- $r^{04}_{1\,-1}$ related to interference between helicity non-flip and double-flip

Interference Effects in Coherent ρ Production

2-source interferometer

- Cannot distinguish γ^* source and target
- ρ production occurs close ($d \lesssim 1\,\mathrm{fm}$) to target nucleus

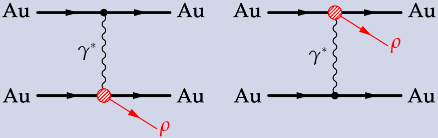

- Interference creates entangled final state $\pi^+\pi^-$ wave function
- $\mathbb{P}(\rho) = -1$: subtract amplitudes

  $$\sigma = \left| A(b,y) - A(b,-y)\, e^{i\vec{p}_T \cdot \vec{b}} \right|^2$$

- For $y \approx 0$: $A(b,y) \approx A(b,-y)$

  $$\implies \sigma = \sigma_0 \left[1 - \cos(\vec{p}_T \cdot \vec{b}) \right]$$

- Suppression at low $p_T \lesssim \hbar / \langle b \rangle$

Klein *et al.*, PL **A308**, 323 (2003)

Interference Effects in Coherent ρ Production

2-source interferometer

- Cannot distinguish γ^* source and target
- ρ production occurs close ($d \lesssim 1\,\text{fm}$) to target nucleus

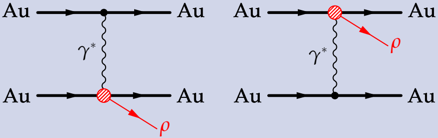

- Interference creates entangled final state $\pi^+\pi^-$ wave function
- $\mathbb{P}(\rho) = -1$: subtract amplitudes

$$\sigma = \left| A(b,y) - A(b,-y)\, e^{i\vec{p}_T\cdot\vec{b}} \right|^2$$

- For $y \approx 0$: $A(b,y) \approx A(b,-y)$

$$\Longrightarrow \quad \sigma = \sigma_0 \left[1 - \cos(\vec{p}_T \cdot \vec{b}) \right]$$

- Suppression at low $p_T \lesssim \hbar / \langle b \rangle$

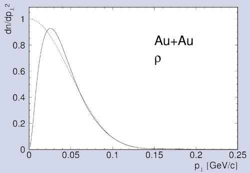

Klein *et al.*, PL **A308**, 323 (2003)

Interference Effects in Coherent ρ Production

Measuring interference in run 2 Au $\times$ Au @ $\sqrt{s_{NN}} = 200$ GeV collisions

- Fit $t(\approx p_T^2)$-spectra with $\frac{\mathrm{d}N}{\mathrm{d}t} = a\, e^{-kt}[1 + c(R(t) - 1)]$
  - k is slope parameter
  - Ratio $R(t) \equiv \frac{t\text{-spectrum with interference}}{t\text{-spectrum without interference}}$ from MC
  - Fit parameter c measures strength of interference
    - $c = 0$ corresponds to no interference
    - $c = 1$ is expected interference
- Different median impact parameters $\tilde{b}$
  - Topology data (no neutron tag): $\tilde{b} \approx 46\,\text{fm}$
  - Minimum bias data (neutron tag): $\tilde{b} \approx 18\,\text{fm}$

  $\Longrightarrow$ interference effects extend to larger p_T
- Energy dependence of ρ production amplitudes decreases interference effect at larger rapidities

Interference Effects in Coherent ρ Production

Run 2 minimum bias data $|y| < 0.5$

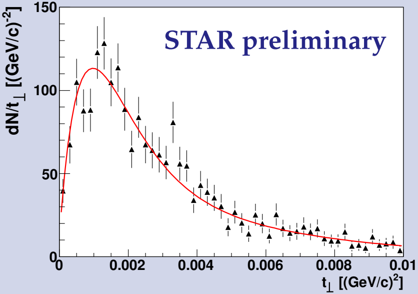

$c = 0.92 \pm 0.07_{\text{stat.}}, \chi^2/\text{ndf} = 45/47$

Run 2 topology data $0.05 < |y| < 0.5$

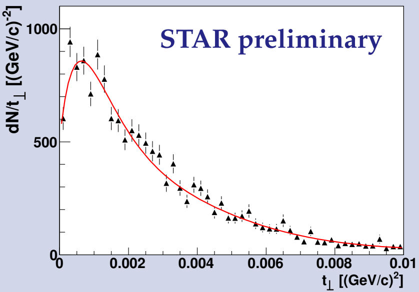

$c = 0.73 \pm 0.10_{\text{stat.}}, \chi^2/\text{ndf} = 53/47$

- Systematic effect due to imperfect trigger simulation

Photonuclear ρ Prod. in d $\times$ Au @ $\sqrt{s_{NN}} = 200\,\text{GeV}$

Asymmetric collision

- γ^* predominantly emitted by Au nucleus
- Topology data
  - Mainly $\gamma^*\,\mathrm{d} \to \rho\,\mathrm{d}$
  - Coherent coupling to entire deuteron
- Topology trigger in coincidence with ZDC neutron signal from deuteron breakup
  - Mainly $\gamma^*\,\mathrm{d} \to \rho\,pn$
  - Coupling to individual nucleons: "incoherent"
- Smaller radii: $R_\mathrm{d} \approx 2\,\mathrm{fm}$, $R_N \approx 0.7\,\mathrm{fm}$ $\Longrightarrow$ ρ has larger p_T

Photonuclear ρ Prod. in d $\times$ Au @ $\sqrt{s_{NN}} = 200$ GeV

Asymmetric collision

- γ^* predominantly emitted by Au nucleus
- Topology data
  - Mainly $\gamma^* \mathrm{d} \to \rho\, \mathrm{d}$
  - Coherent coupling to entire deuteron
- Topology trigger in coincidence with ZDC neutron signal from deuteron breakup
  - Mainly $\gamma^* \mathrm{d} \to \rho\, pn$
  - Coupling to individual nucleons: "incoherent"
- Smaller radii: $R_\mathrm{d} \approx 2$ fm, $R_N \approx 0.7$ fm $\Longrightarrow$ ρ has larger p_T

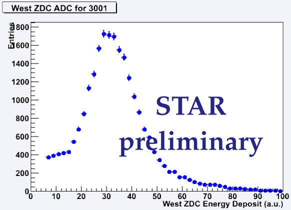

Neutron tagged data

Photonuclear ρ Prod. in d $\times$ Au @ $\sqrt{s_{NN}} = 200\,\text{GeV}$

Asymmetric collision

- γ^* predominantly emitted by Au nucleus
- Topology data
  - Mainly $\gamma^*\,\text{d} \to \rho\,\text{d}$
  - Coherent coupling to entire deuteron
- Topology trigger in coincidence with ZDC neutron signal from deuteron breakup
  - Mainly $\gamma^*\,\text{d} \to \rho\, pn$
  - Coupling to individual nucleons: "incoherent"
- Smaller radii: $R_\text{d} \approx 2\,\text{fm}$, $R_N \approx 0.7\,\text{fm}$
  $\Longrightarrow$ ρ has larger p_T

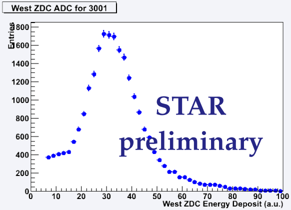

Neutron tagged data

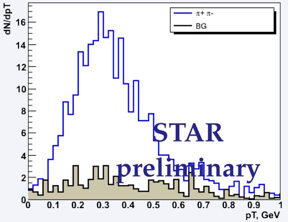

Photonuclear ρ Prod. in d $\times$ Au @ $\sqrt{s_{NN}} = 200$ GeV

t-spectrum for d-breakup (“incoherent”)

- Exponential fit function: $\mathrm{d}N/\mathrm{d}t = a\,e^{-kt}$
- Slope parameter
  $k = 9.06 \pm 0.85_{\text{stat.}}\ \text{GeV}^{-2}$
  - Related to nucleon form factor
  - Similar to results from
    Au $\times$ Au @ $\sqrt{s_{NN}} = 200$ GeV :
    $k = 8.8 \pm 1.0_{\text{stat.}}\ \text{GeV}^{-2}$
    PR **C77**, 034910 (2008)
  - Compatible with ZEUS
    $k = 10.9 \pm 0.3_{\text{stat.}}\ {}^{+1.0}_{-0.5}\,{}_{\text{syst.}}\ \text{GeV}^{-2}$
    EPJ **C2**, 247 (1998)
- Downturn at low t
  - Not enough energy for d dissociation
  - Also seen in low-energy γd (SLAC 4.3 GeV   Eisenberg *et al.*, NP **B104**, 61 (1976))

Neutron tagged data

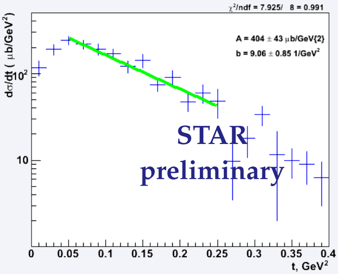

$t \approx t_{\perp} = p_T^2$

$\pi^+\pi^-\pi^+\pi^-$ Production in Au $\times$ Au @ $\sqrt{s_{NN}} = 200$ GeV

Photonuclear production with mutual nuclear excitation

- Run 4: 3.9 M multi-prong triggers
  - Coincident neutrons from nuclear breakup in both ZDCs
  - Low CTB multiplicity
  - Veto from large-tile BBCs

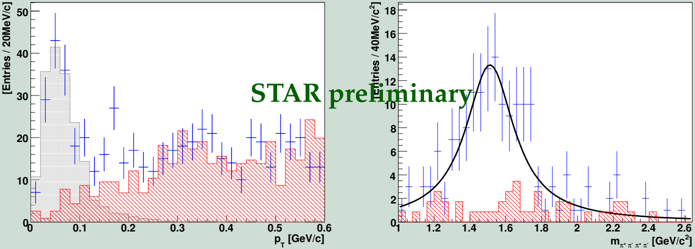

- Peak: 123 events at $m = (1510 \pm 20)$ MeV/c^2, $\Gamma = (330 \pm 45)$ MeV
- Could be $\rho(1450)$ and/or $\rho(1700)$

e^+e^--Pair Production in Au $\times$ Au @ $\sqrt{s_{NN}} = 200$ GeV

Strong electromagnetic fields

- $Z\alpha \approx 0.6 \implies$ conventional perturbative calculations may be questionable
- Enrich collisions at small impact parameters (= stronger fields) by requiring mutual Coulomb excitation $2R_A < b \lesssim 30\,\mathrm{fm}$

Run 2 minimum bias data

- Challenging measurement due to small acceptance
- Most $e^\pm$ produced at very low p_T
  - Reconstructible only at half solenoid field of 0.25 T
- $e^\pm$ identification via $\mathrm{d}E/\mathrm{d}x$ in TPC gas
  - Clean sample with PID efficiency close to 1 and minimum contaminations for $p_{e^\pm} < 130\ \mathrm{MeV}/c$
- Limited statistics: 52 events

e^+e^--Pair Production in Au $\times$ Au @ $\sqrt{s_{NN}} = 200$ GeV

Differential cross sections $d\sigma/dM_{e^+e^-}$ and $d\sigma/dp_T^{e^+e^-}$

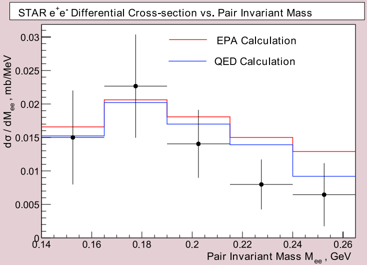

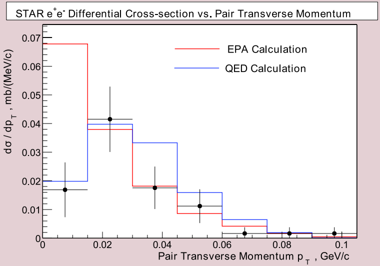

- Data compared with 2 models:
  - **EPA**: equivalent photon approach — PR **C70**, 031902 (2004)
    - Treats γ^* as real photons
    - Fails for lowest p_T bin ($p_T < 15$ MeV/c)
  - **QED**: lowest order QED calculation with simplified model for Coulomb excitation (GDR only) — Henken *et al.*, PR **C69**, 054902 (2004)
    - Describes data well

e^+e^--Pair Production in Au $\times$ Au @ $\sqrt{s_{NN}} = 200$ GeV

New QED calculation with realistic phenomenological treatment of Coulomb excitation

Baltz, PRL **100**, 062302 (2008)

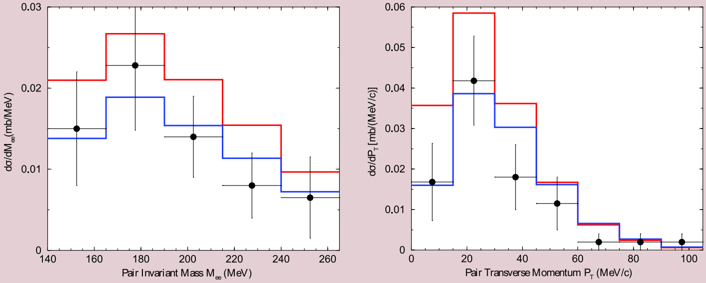

- **Lowest order QED**
  - Overshoots data
    $\sigma_{\text{QED}} = 2.34\,\text{mb}$ vs. $\sigma_{\text{exp}} = 1.6 \pm 0.2_{\text{stat.}} \pm 0.3_{\text{syst.}}\,\text{mb}$
- **Including higher order corrections**
  - Good agreement with data, $\sigma_{\text{QED}} = 1.67\,\text{mb}$